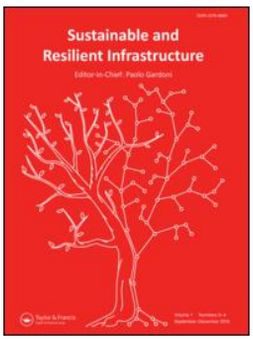

Taylor & Francis
Taylor & Francis Group

Sustainable and Resilient Infrastructure

ISSN: 2378-9689 (Print) 2378-9697 (Online) Journal homepage: https://www.tandfonline.com/loi/tsri20

Influence of geometric parameters on the restraint of guardrail posts by asphalt mow strips

Seo-Hun Lee, Esmaeel Bakhtiary, David W. Scott, Lauren K. Stewart & Donald W. White

To cite this article: Seo-Hun Lee, Esmaeel Bakhtiary, David W. Scott, Lauren K. Stewart & Donald W. White (2017) Influence of geometric parameters on the restraint of guardrail posts by asphalt mow strips, Sustainable and Resilient Infrastructure, 2:1, 22-36, DOI: 10.1080/23789689.2017.1278993

To link to this article: https://doi.org/10.1080/23789689.2017.1278993

SUSTAINABLE AND RESILIENT INFRASTRUCTURE, 2017
VOL. 2, NO. 1, 22–36
http://dx.doi.org/10.1080/23789689.2017.1278993

Taylor & Francis
Taylor & Francis Group

Influence of geometric parameters on the restraint of guardrail posts by asphalt mow strips

Seo-Hun Lee, Esmaeel Bakhtiary, David W. Scott, Lauren K. Stewart and Donald W. White

School of Civil and Environmental Engineering, Georgia Institute of Technology, Atlanta, GA, USA

ABSTRACT

Asphalt pavement mow strips, used as a vegetation barrier in guardrail systems, have typically been regarded as a rigid layer in roadside design. However, geometric parameters of the mow strip such as thickness and rear distance behind the post have a significant impact on the amount of restraint the asphalt layer provides to resist translation and rotation by the posts. In this paper, a standard steel guardrail post designed with a range of asphalt mow strip dimensions is evaluated. A survey of the use of asphalt pavement mow strips in the United States was undertaken to determine an initial set of mow strip designs for investigation. Static tests were performed based on these designs, and finite element models were calibrated using the test data and parallel material characterization experiments. Utilizing the calibrated finite element model, simulations were performed on a wide variety of asphalt mow strip designs. Simulation and experimental results were correlated to develop a set of quantitative performance criteria. These criteria were used to assess the amount of ground-level restraint on a guardrail post caused by a given asphalt mow strip design in comparison with the existing design recommended by American Association of State Highway and Transportation Officials.

ARTICLE HISTORY
Received 19 February 2016
Accepted 2 August 2016

KEYWORDS
Guardrail post; asphalt mow strip; parametric study; static test; finite element simulation

Introduction

Asphalt mow strips are a pavement layer installed around guardrail posts as a vegetation barrier. Without a mow strip, regular vegetation control around the guardrail such as mowing or herbicide application is required to prevent vegetation growth. Prior research (Bligh et al., 2004) has concluded that asphalt mow strips increase the ground-level restraint of guardrail posts significantly. Therefore, the American Association of State Highway and Transportation Officials (referred to hereafter as 'AASHTO') Roadside Design Guide (American Association of State Highway and Transportation Officials [AASHTO], 2011) classifies mow strips as rigid foundations and states that guardrail posts in mow strips are not able to rotate in the soil. However, other researchers have reported that asphalt strength and other material properties of the mow strip are sensitive to the temperature (Fwa, Tan, & Zhu, 2004; Zhang, Luo, & Lytton, 2013) and age (Bell, 1989; Farrar, Turner, Planche, Schabron, & Harnsberger, 2013), which contradicts the assumption of asphalt as a 'rigid' material.

In addition, Bligh et al. (2004) have shown that steel guardrail posts confined in asphalt will exhibit the sudden development of a plastic hinge during a vehicle impact, which is not a desirable performance in guardrail systems. As a solution to this issue, the Roadside Design Guide recommends using a leave-out, where the portion of the mow strip around the post is removed and replaced by a relatively weak material (e.g. low-strength cementitious grout) to reduce the ground-level restraint on the post-mow strip system (Figure 1). While generally effective, installing a leave-out requires more time and cost compared to the typical post-driven mow strip installed by machine. This can be attributed to the additional construction processes needed such as the removal of mow strip around the posts and the preparation/placement of leave-out materials.

A large volume of studies have addressed the performance of the strong-post W-beam guardrail systems including full-scale dynamic tests and finite element simulations (Ferdous, Abu-Odeh, Bligh, Jones, & Sheikh, 2011; Mak, Bligh, & Menges, 1998; Plaxico, Ray, & Hiranmayee, 2000; Sicking, Reid, & Rohde, 2002). The performance was evaluated based on the guidelines provided in NCHRP

CONTACT David W. Scott dscott@gatech.edu

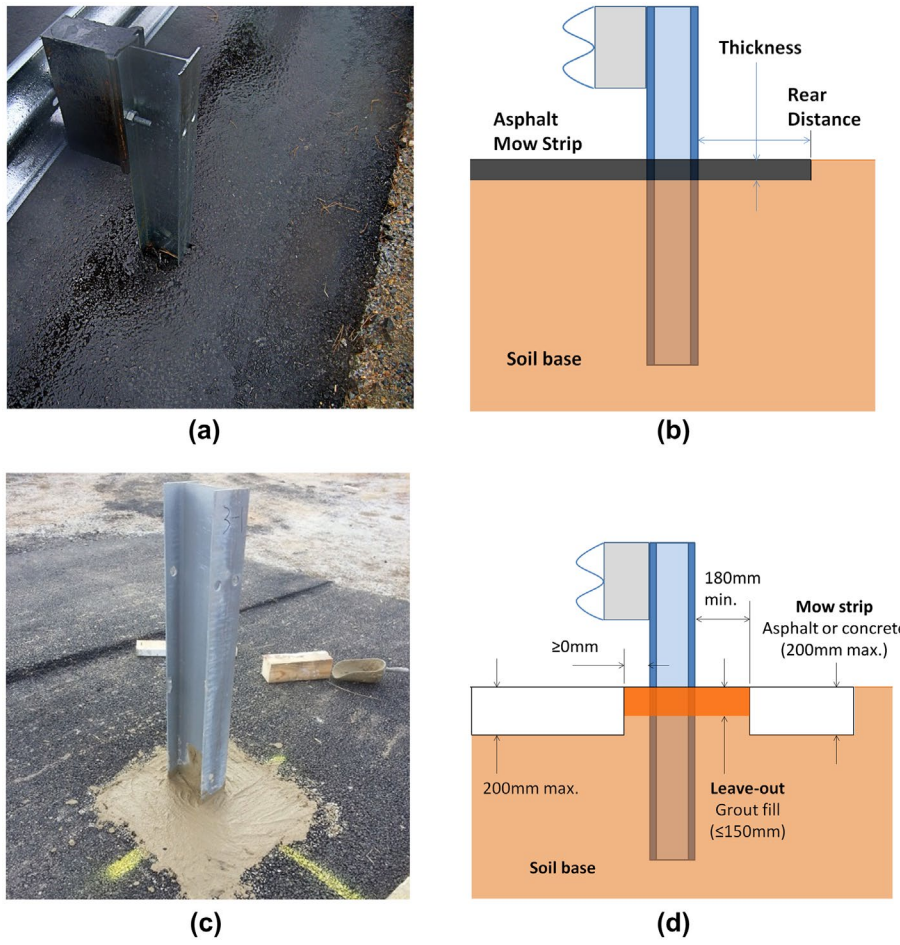

Figure 1. Typical guardrail post installation: (a) asphalt mow strip, (b) mow strip geometric parameters (after Georgia Department of Transportation, 2015), (c) grout-filled leave-out, and (d) recommended leave-out dimension.

Report 350 (Ross, Sicking, Zimmer, & Michie, 1993) and Manual for Assessing Safety Hardware (referred to hereafter as 'MASH') (AASHTO, 2009). Nonetheless, only a few studies have been performed which incorporate a mow strip. Particularly, the study performed by the Texas Transportation Institute (Bligh et al., 2004) examined the performance of guardrail systems with various embedment conditions of posts by changing the dimensions and materials of the mow strips and leave-outs. The research formed the basis for the adoption of the guardrail post installation details incorporating grout leave-outs into the Roadside Design Guide, as well as for two subsequent studies of focusing primarily on alternative leave-out materials (Arrington, Bligh, & Menges, 2009; Whitesel, Jewell, & Meline, 2011).

The previous studies, which focused solely on the performance of the leave-out design, did not consider the performance and optimization of alternative methods to reduce ground-level restraint. Consideration of other methods may provide designs that have both sufficient reductions in ground-level restraint and better constructability. For example, less ground-level restraint can be achieved by reducing two geometric parameters of the mow strip: thickness and rear distance (as shown in Figure 1). This paper provides a fundamental evaluation of the guardrail post ground-level restraint by asphalt mow strips with various geometric parameters.

Scope of research

MASH Appendix D specifies a static test as one of experimental tools to compare the performance of competing design details of guardrail system (AASHTO, 2009). Previous studies have shown that static subcomponent tests can be used for performance evaluation in the preliminary development of guardrail systems (Dewey, Jeyapalan, Hirsch, & Ross, 1983; Eggers & Hirsch, 1986). It is well known that static testing cannot fully replace dynamic full-scale testing in evaluating the performance of guardrail systems. However, static tests are an economical alternative in making an initial comparison of the relative performance of posts installed with various configurations of mow strips, particularly in comparison to the static performance of a mow strip with a leave-out.

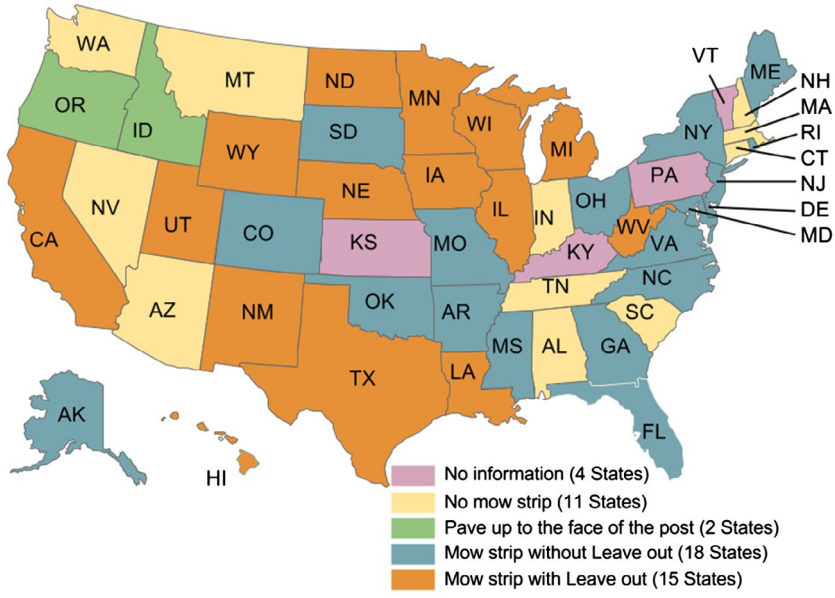

Figure 2. Asphalt mow strip configuration by state based on 2015 survey of current state of practice.

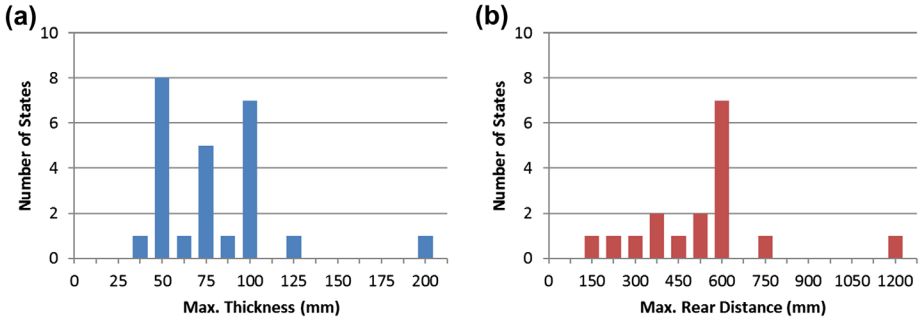

Figure 3. Asphalt mow strip geometric parameters found in state DOT databases: (a) maximum thickness, and (b) maximum rear distance.

This initial evaluation can narrow the required scope of costlier follow-on subcomponent and full-scale dynamic testing. The correlation of static experimental results and finite element simulation can also allow some degree of parametric study of critical geometric variables and alternatives in the design and installation of the vegetation barriers. The work presented here reports the results of this phase of the overall research program. The results of dynamic testing and the correlation of the static test results to observed dynamic performance will be presented at a later time.

It is well known that asphalt materials exhibit viscoelastic behavior that significantly influences its response to sustained loading (Thom, 2013). This is a significant factor when evaluating the in-service performance of asphalt roadways to avoid deterioration mechanisms such as rutting (AASHTO, 1993). However, the viscoelastic nature of the material is less of a factor under impact forces such as those in a traffic accident. As such, the time-dependent behavior of the asphalt was not specifically evaluated during the pseudo-static test program.

The significant influence of aging and service temperature on asphalt performance (e.g. resilient modulus) has also been extensively studied (Bell, 1989; Farrar et al., 2013; Fwa et al., 2004; Zhang et al., 2013). However, the testing schedule for work presented here did not allow for delays to examine the effects of physical aging over a time-scale of significance. Also, researchers were limited by the schedule and location of the test bed in effectively evaluating the effect of service temperatures on the performance of the post system. More details related to the examination of aging and temperature on the performance of the guardrail posts in these experiments may be found in Scott, White, Stewart, Bakhtiary, and Lee (2015).

Current state of practice

To identify alternatives to the typical leave-out design/configuration, it was first necessary to study the current state of practice related to the use of asphalt vegetation barriers in the United States. Publically accessible websites were investigated, and phone solicitations were performed

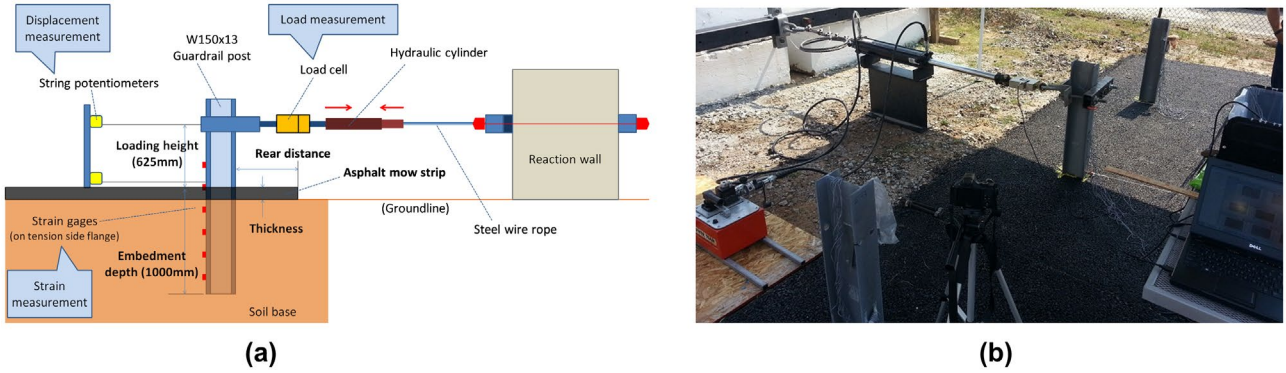

Figure 4. Experimental test: (a) setup, and (b) site picture.

Table 1. Sieve analysis for test soil.

AASHTO M147 grading requirements			Test soil	
Sieve size (mm)	Sieve designation	Grade B criteria: mass passing (%)	Test results: mass passing (%)	Assessment
50	2 in.	100	100	Pass
25	1 in.	75–95	91.7	Pass
9.5	3/4 in.	40–75	59.8	Pass
4.75	No. 4	30–60	47.4	Pass
2.00	No. 10	20–45	36.7	Pass
.425	No. 40	15–30	25.0	Pass
.075	No. 200	5–20	7.73	Pass

for all 50 state Departments of Transportation (DOT). Based on the obtained information, it was determined that 11 states currently do not use mow strips, 18 states use mow strips without incorporating a leave-out, and 15 states use mow strips including a leave-out. No information was found for four states, and two states stated that their practice is to pave up to the face of the post. Based on the information gathered as of July 2015, there does not appear to be a significant correlation between geographic location and the current state of practice for mow strip usage as shown in Figure 2 (Scott, Lee, Bakhtiary, Arson, & White, 2015; Scott, White, et al., 2015).

The range of asphalt mow strip geometric parameters employed in mow strip designs was also investigated. Figure 3 shows a summary of maximum thickness and rear distance acquired from the survey. From the 25 states where the highest thickness of mow strip is specified, the thickness ranges from 37.5 to 200 mm, with a nationwide average of 79.5 mm, median of 75 mm, and mode of 50 mm. Similarly, from the 17 states where the maximum rear distance of mow strip is specified, the rear distance ranges from 150 to 1200 mm, with a nationwide average of 534 mm, median of 600 mm, and mode of 600 mm. These ranges were used in developing the test matrix and the parametric study plan of finite element simulation.

Experimental setup

Figure 4 shows the static test setup including the loading fixture and instrumentation.

Soil, asphalt, and steel post installation

The soil in the test bed was prepared with graded base coarse aggregates to meet AASHTO M147 grading A/B requirements (AASHTO, 2012b) in accordance with MASH guidelines (AASHTO, 2009). Sieve analysis for the test bed soil was performed, and the results are shown in Table 1. The soil was classified as A-1-a (stone fragments, gravel, and sand) by the AASHTO Soil-Aggregate Classification System (AASHTO, 2012a). A maximum dry density 22.7 kN/m^3 of the soil was determined by the laboratory soil tests. Prior to each test, the soil was compacted to exceed 95% of the maximum dry density of soil.

The same type of hot mixed asphalt (HMA), classified as PG 76-22 binder and 19 mm aggregate size, was installed as a mow strip for each test. This type of HMA was recommended for use in the testing program by the Georgia Department of Transportation (GDOT) as it is one of the more commonly used paving materials in the state of Georgia. Approximately one week after the asphalt installation, W150 × 13 (W6 × 9) steel guardrail posts were driven through the asphalt layer (if present) and into the ground by blows from a hydraulic post driver provided by the GDOT. The time duration of each post installation was less than 2 min.

Test description

A lateral load on the guardrail post was applied by the retraction of the hydraulic cylinder. Lateral load on the

Table 2. Experimental test matrix.

Test number	Mow strip thickness (mm)	Mow strip rear distance (mm)	Test temperature (°C)	Asphalt age (day)	Note
B1, B2, B3	0	0	26	–	Baseline
T1, T2	50	600	32	18	Typical mow strip geometry
T3	50	600	10	118	(two thicknesses)
T4	50	600	24	40	
T5, T6	90	600	32	18	
T7	90	600	10	118	
L1, L2	90	600	24	40	Leave-out around the post
L3	90	600	22	32	(450 mm × 450 mm)
R1	50	150	24	40	Reduced rear distance
R2	50	300	24	40	
R3	90	300	22	32	

Table 3. Material constants used in the finite element model.

Material	Constitutive parameter	Value	Determined from
Steel	Density, ρ	7930 kg/m^3	Material test
	Young modulus, E	200 GPa	Bligh et al. (2004)
	Poisson's ratio, ν	.3	Bligh et al. (2004)
	Yield strength, σ_y	348 MPa	Material test
Soil	Density, ρ	2300 kg/m^3	Material test
	Cohesion, C	13 kPa	Material test and via system test calibration[a]
	Peak friction angle, ϕ'_p	45°	Material test and via system test calibration[a]
	Critical friction angle, ϕ'_{cr}	15°	Budhu (2010) and via system test calibration[a]
	Shear modulus, G	50 MPa	USACE (1982) and via system test calibration[a]
	Poisson's ratio, ν	.25	Bowles (1996)
	Density, ρ	2300 kg/m^3	Material test
	Cohesion, C	500 kPa	Material test
	Friction angle, ϕ'	35°	Christensen and Bonaquist (2004))
Asphalt	Shear modulus, G	50 MPa	Via system test calibration[a]
	Poisson's ratio, ν	.35	Pellinen, Song, and Xiao (2004)
	Maximum principle stress, σ_{max}	680 kPa	$\sigma_{max} = .95C/\tan(\phi)$
	Maximum principle strain, ε_{max}	.07	Via system test calibration[a]

[a]The term 'system test calibration' refers to the selection of certain material constants based on one selected system test as described above.

post, displacement of the post, and longitudinal strains along the post flange were measured and recorded through a data acquisition system. A load cell was linked with the retracting arm of the hydraulic cylinder and with a loading bracket transmitting the lateral load to the post. During each test, the hydraulic cylinder was used to apply a lateral load on the guardrail post at a rate of approximately 1 mm/s.

Threaded bearing rods were attached on both sides of the load cell to prevent bending and torsion along the load axis. Two string potentiometers were mounted on a reference pole with a stand-off distance of approximately 1.8 m from the post. One string potentiometer measured the lateral displacement at the level of the loading (625 mm from ground level) and one measured the displacement at the ground level. Nine strain gauges, attached to the tension side flange of each guardrail post, measured the longitudinal strain from 750 mm below the ground level to 250 mm above the ground level. A metal shim was attached at the bottom of the flange and covered all gages and wires under the ground level to prevent the damage from post-driving.

Table 2 outlines the test matrix for the experimental program including the test information of 16 guardrail posts: the test configuration and test condition (temperature, asphalt age, etc.). The first three tests (B1–3) were designated as the baseline configuration, which were used to calibrate the finite element model without the asphalt mow strip. The next seven tests (T1–7) were mow strip configurations commonly used by state DOT organizations, which were used to calibrate the finite element model with mow strip, acknowledging the influence of temperature and age condition of the asphalt. The final six tests consist of three typical leave-out-applied configurations (L1–3) and three reduced rear distance settings (R1–3). The 28-day compressive strengths of the grout materials used in leave-out were less than .83 MPa (120 psi), which satisfied the recommendation in the Roadside Design Guide (AASHTO, 2011).

Finite element model description

It is often not cost-effective to perform full-scale experimental tests on an entirely comprehensive set of parameters. Simulation of guardrail posts using nonlinear FEA is an effective way to assess these systems. Three-dimensional FEA was utilized in this research to calculate the guardrail post response subject to static loading. The

model presented in this paper was developed via a combination of selecting material constants based on commonly accepted values, material testing, and calibration using system testing. Once the model was calibrated at the system level, the material properties and other model parameters (e.g. loading rate and contacts) were kept constant. Then the performance and accuracy of the model were evaluated by comparing results from the model with further experimental tests before being used independently to conduct parametric studies.

The FEA studies were conducted using LS-DYNA® V971 R8.0.0 (Livermore Software Technology Corporation [LSTC], 2014). The quasi-static problem was solved with explicit instead of implicit time integration. The model developed for the present work will be revised for use with both subcomponent and full-scale dynamic testing. Therefore, optimizing the model for implicit integration is not useful. Moreover, the Mohr–Coulomb material model which is used to model soil and asphalt does not support implicit time integration and large strains. Lastly, the contact models and solution algorithms are less robust with implicit time integration.

Lateral loading in the static test program was simulated as follows. A transverse displacement was applied to the post at 625 mm above the ground level. Mass scaling was not used, and the rate of displacement of the post was varied between 5000 and 25 mm/s. Analysis of the results showed that rates slower than 50 mm/s gave results within 1% for all the primary response quantities. Therefore, 50 mm/s was used as the displacement rate of the post to represent quasi-static loading. The kinetic energy of the system was checked and determined to be less than .5% of the total energy. The simulation time using 6 CPUs at 3.5 GHz is approximately 24 h; this duration changes when the asphalt geometric parameters such as thickness and rear distance are changed.

The soil domain considered in the model is a rectangular prism. The bottom boundary of the prism was fixed at a depth (z-direction) of 2 m (twice the embedment depth of the post), and the nodes on the lateral boundary were initially set free. The planar size of the prism was increased until the displacements of the nodes on the boundaries were less than 1% of the ground level displacement of the steel post. The planar dimensions of the prism were obtained as 5 m in the y-direction (parallel to the post lateral movement) and 10 m in the x-direction (perpendicular to the post lateral movement, and doubled to capture lateral asphalt rupture properly).

For the lateral boundaries, there are three options to use: free, rigid, or non-reflecting boundary conditions. The lateral boundaries are far enough from the post such that the displacements and change of stresses at the boundaries are negligible, and the response is insensitive to the lateral boundary assumptions. For the pseudo-static loading employed, the non-reflecting boundary conditions are essentially the same as the free boundary conditions. Therefore, using any of these three boundary conditions gives virtually the same results. However, non-reflecting boundaries are used in the model to simulate actual conditions in a large volume of soil and to slightly decrease noise in the system response.

Gravity is applied using a body load in the z-direction. Dynamic relaxation is a useful technique available in LS-DYNA for applying initial gravity loading conditions prior to the time when transient loadings are applied. This technique is used in the model before transient analysis to avoid any oscillations due to the application of gravity. The stress in the z-direction was checked for the elements at the bottom of the soil model to confirm that the overburden stress is accurately calculated based on the depth of the soil and its density. Dynamic relaxation is separate from applying a general damping to the model in the time when transient loads are applied. Dynamic relaxation, as defined in LS-DYNA, is not a viable option during the static loading phase when strains are large. A general damping was considered for use during the transient time, but it did not substantially reduce noise at the frequencies seen in the response.

Fully integrated shell elements with nine integration points through the thickness and a uniform structured mesh with a size of 25 mm are used for the steel post. Using an element size of 12 mm within the steel post increases the peak force applied to the post approximately 5%. The ground level displacement decreases approximately 7%. These changes occur because using a finer mesh provides greater resolution in capturing local deformation of the post. However, using the finer mesh increases the simulation time by approximately 100%. Thus, the 25 mm element size was considered sufficient. The soil is modeled using structured hexahedral constant stress solid elements. The final mesh size for soil changes from 25 mm close to the post to 200 mm at locations far from the post. Using a mesh in the soil finer than approximately 25 mm caused instability in the model.

Enhanced assumed strain stiffness form for 3D hexahedral elements hourglass control (number 9) was used for the soil elements and the hexahedral mesh part of the asphalt to prevent high hourglass energy during simulations. Hourglass coefficients equal to .004 and .1 were used for the soil elements and the hexahedral mesh part of the asphalt, respectively. Because of the type of the elements used for the steel post and tetrahedral mesh part of the asphalt, these two parts do not have any hourglass energy and do not need an hourglass control. Hourglass energy was monitored and compared with the internal energy. The hourglass energy in the soil and the hexahedral mesh

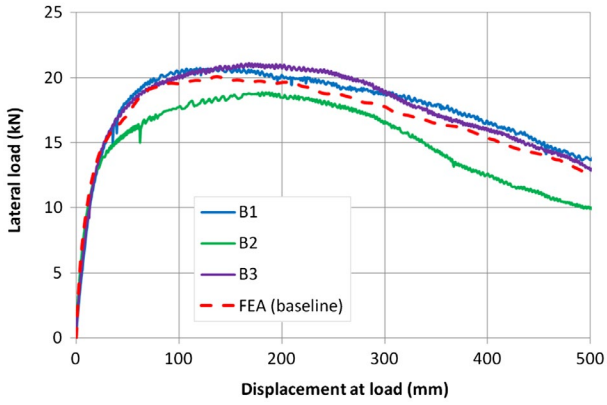

Figure 5. Comparison of load-displacement curves for the baseline model.

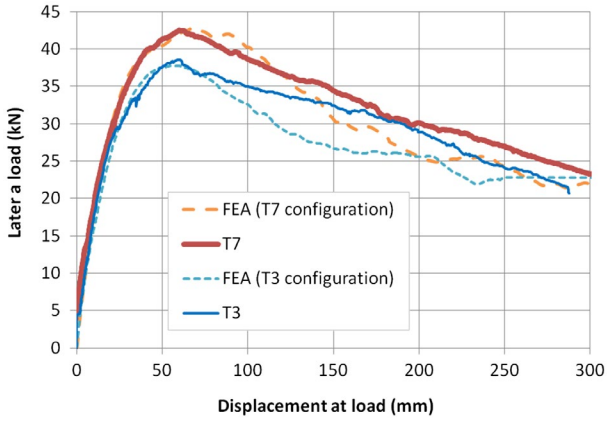

Figure 6. Comparison of load-displacement curves for configurations with asphalt mow strip.

part of the asphalt were less than 3% of the internal energy, which is acceptable.

The contacts between the soil and the steel post, the soil and the asphalt, and the asphalt and the steel post are modeled using automatic surface-to-surface contact. Static and dynamic friction coefficients for the interface between soil (a mixture of gravel, sand, and clay) and the driven smooth steel post was obtained as .6 (Kulhawy, O'Rourke, Stewart, & Beech, 1983) and this value was used in the model. The sliding energy was always positive during simulations, which confirms that the contact definitions were performing properly. The contact forces between the post and the soil, and between the post and the asphalt layer in the y-direction were calculated by the model to determine the applied force vs. displacement curve. For the cases including a mow strip discussed below, evaluating the contact forces between the post and the soil and mow strip allows direct evaluation of the separate forces contributed from the soil and from the mow strip.

The constitutive model for the elements representing the post is piecewise linear plasticity. Density of the steel equal to 7930 kg/m^3, yield strength equal to 348 MPa, and an experimental stress–strain curve using tension tests on samples from guardrail posts were obtained. This curve is utilized in the model and accounts for the strain hardening. Common steel parameters are used for Young's modulus (E) equal to 200 GPa and Poisson's ratio (v) equal to .3 (Bligh et al., 2004). The steel material constants and the procedure to determine them are summarized in Table 3. The Mohr–Coulomb material model is used for asphalt and soil. The Mohr–Coulomb yield condition may be expressed as:

$$\tau = c + \sigma \tan(\phi) \quad (1)$$

where τ is the shear stress, σ is the normal stress, c is the cohesion, and ϕ is the friction angle of the material.

Calibration of the finite element model

Soil

Based on the laboratory test on soil samples, the density of the soil was approximately 2300 kg/m^3. This value was used as the soil density in the numerical modeling. Soil grain size distribution was determined from laboratory tests, and the soil type was determined as poorly graded gravel with silt and sand using the Unified Soil Classification System. Lekarp, Richardson, and Dawson (1996) determined Mohr–Coulomb material parameters using laboratory tests on soil specimens for different subbase materials used in pavement structures. They obtained the C parameter and peak friction angle ϕ for a sandy subbase equal to 9.8 kPa and 49°, respectively. These values were initially used in the model and then the model was calibrated to capture the peak applied force and the displacement at which the peak force occurs in the load-displacement response of the system. After the calibration, values of 9 kPa and 45° were found for the cohesion C and peak friction angle ϕ, respectively, which are in the range of recommended values for gravel with silt and sand used as subbase material (Budhu, 2010). The small value of C was expected for a coarse grain soil since C represents the apparent soil cohesion which is typically associated with strength due to suction in fine grain soils. In addition to the system calibration of soil material properties, direct shear tests were performed on a limited number of soil samples obtained from the system test site. Cohesion and peak friction angle were estimated at approximately 7 kPa and 50°, respectively. These test results indicate that the values used for peak friction angle and cohesion in the model after calibration are a reasonable representation of the soil used in the experiments.

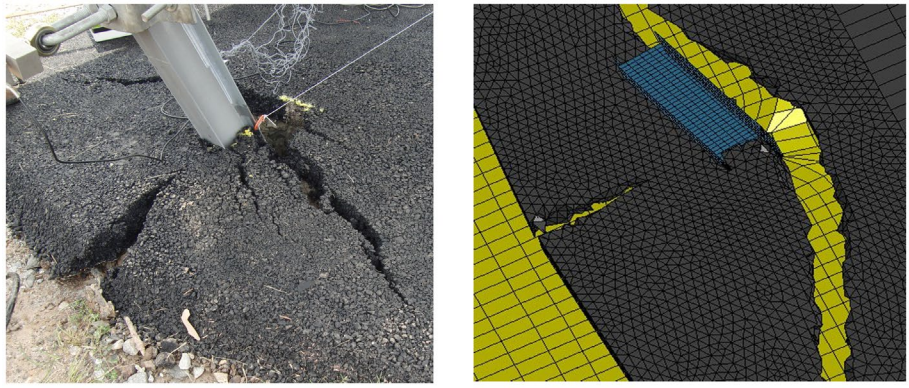

Figure 7. Comparison of asphalt rupture: (a) in the experiment, and (b) in FEA simulation.

The peak friction angle in dense soils with coarse grains is typically higher than the critical friction angle. This is due to dilation. To account for dilation and the change of friction angle, a trilinear curve was specified to define the friction angle of the Mohr–Coulomb material model as a function of the effective plastic strain. The friction angle equals 45° for plastic strain values less than .4 and linearly decreases to .15 between the plastic strains of .4 and .5. For plastic strains greater than .5, the friction angle equals 15°.

A standard value of .25 was used for the Poisson's ratio that is typical for the mixture of gravel, coarse sand, and silt (Bowles, 1996). The initial linear elastic portion of the load-displacement curve was used to calibrate the shear modulus equal to 50 MPa, which is in the common range of values for the soil type used in this research (United States Army Corps of Engineers [USACE], 1982). The numerical load-displacement curve after the calibration is compared to the experimental load-displacement curve as shown in Figure 5. A point average filter was used to remove high-frequency noise in the FEA simulation result. It can be observed that the simulation results show good agreement with the experimental curves.

Based on experimental tests on setups with finite rear distance, one part of the asphalt detaches from the rest of it after the rupture propagates in the asphalt. After this point, the only resisting force for large deformations is from the soil. Therefore, as presented in Figure 6, two mow strip systems with different thicknesses provide similar force response for displacements more than 200 mm. When the part of the curves after 200 mm displacement is compared between Figures 5 and 6, it can be seen that the soil in the systems with mow strips shows higher strength. Therefore, the *C* parameter for soil was increased to 13 kPa to scale up the soil strength and account for the increase of soil strength due to asphalt compaction and moisture being trapped in the soil by the asphalt cover. The soil material constants and the procedure to determine them are summarized in Table 3.

Asphalt

As the shear strength of asphalt is known to be pressure dependent, Mohr–Coulomb and Drucker–Prager material models are widely used to model the material (Zhang et al., 2013). In this research, the Mohr–Coulomb material model was chosen to model the shear strength of the asphalt mow strip. A set of material properties of asphalt was estimated using laboratory test data. The density of the asphalt was estimated to be 2300 kg/m^3 using laboratory tests. The cohesion was estimated to be 500 kPa using experimental unconfined compression tests on asphalt specimens. Another set of material properties of asphalt was calibrated using load-displacement responses of representative post-mow strip system. Since the cohesion and the shear modulus of elasticity asphalt increase in lower ambient temperature and older age condition (Farrar et al., 2013; Fwa et al., 2004), experimental results of tests T3 and T7, performed at the lowest ambient temperature of 10 °C and the oldest age condition of 118 days among all test dates, were used in the model calibration so that the calibrated FE model might conservatively evaluate the performance of alternative mow strip design. The shear modulus of elasticity was set to 50 MPa using the early linear-elastic portion of the load-displacement curve. The Poisson's ratio and friction angle of the asphalt were specified as .35 and 35° through the model calibration, respectively. These parameters were kept constant for all parametric studies on mow strip geometry.

The tensile rupture in the asphalt layer observed in the experimental tests was modeled as follows. When an element fails by rupture, it loses stiffness and is removed from the computations. This was done in the FEA software using an element erosion approach (LSTC, 2014). Element erosion can be done through the material model by including erosion criteria in the material model's formulation. Another way to apply element erosion is using general element erosion criteria for solid elements. Each

criterion is applied independently, and satisfaction of one or more criteria causes deletion of an element from the calculations. The number of erosion criteria, which must be satisfied before an element is removed, can be specified by the user. General element erosion criteria for solid elements were utilized in this research. The criteria for failure employed were:

- $\sigma_1 \geq \sigma_{max}$ where σ_{max} is the failure principle stress and σ_1 is the current maximum principal stress.
- $\varepsilon_1 \geq \varepsilon_{max}$ where ε_{max} is the failure principal strain and ε_1 is the current maximum principal strain.

The maximum principal stress criterion was used to remove the elements when the tensile failure criterion was met. However, the rupture in the asphalt was abrupt when solely this criterion was used, and the strength decreased dramatically similar to what is commonly observed in very brittle materials. To account for the fact that asphalt is not as brittle as a rock (for example) and can accommodate larger strains before failing under tensile stress, an additional maximum principle strain failure criterion was added to the material model. Therefore, an element was removed when both the maximum principal stress criterion and the principal strain criterion were satisfied. The maximum principle stress at failure can be obtained using Mohr–Coulomb yield criterion as $.95C/\tan(\phi')$ equal to 680 kPa. A reduction factor of .95 was chosen to facilitate proper element erosion. By calibrating the post-peak response of the system, the maximum principle strain at failure was obtained as .07. The asphalt's material constants and the way they were determined are summarized in Table 3.

For the asphalt, the mesh around the post is composed of unstructured tetrahedral elements with one-point integration to better capture asphalt rupture propagation and element erosion. The average size of the mesh is approximately 25 mm. Principle strain at failure, which is used for asphalt element erosion, is mesh size dependent. The rupture propagates faster with a finer mesh and slower with a coarser mesh. Using a much coarser or much finer mesh (as large as two times coarser or finer) for this part of the asphalt requires a different value for the principle strain at failure which requires calibration. Hexahedral constant stress solid elements are used to model the asphalt not within the vicinity of the post. Larger size elements were used at further distances from the post to reduced computational cost. Moreover, hexahedral elements are less stiff than tetrahedral elements. The two different asphalt meshes are connected to make a continuum part for the asphalt using a tied surface to surface contact model.

A comparison between the results achieved from the FEA simulation and two experimental tests (T3 and T7) is presented in Figures 6 and 7. Figure 7 shows a visual comparison of rupture in asphalt mow strip between the observation in the experiment and the FEA results. Similar responses were observed from the appearance and propagation of tensile cracks in the asphalt layer. Figure 6 compares two experimental load-displacement curves, measured from asphalt mow strip configurations of 90 and 50 mm thick, with other two curves from the FEA simulation on identical configuration. In both configurations, these experimental curves show a reasonable agreement with the analysis results. Then the asphalt and soil parameters were held constant, and the results from the model were compared with experimental tests on guardrail posts with mow strips with various thicknesses and rear distances. The model proved able to produce reasonable results independently and was used to predict further experimental test results and conduct parametric studies.

Finite element parametric studies

Changing asphalt mow strip geometry influences post-mow strip system performance. As the thickness and the rear distance behind the post increase, the ground-level restraint of the asphalt layer on the post-mow strip system increases. Parametric studies on the combination of different thicknesses and rear distances were a critical step to explore the impact of each of these parameters. The common asphalt thickness used in the state of Georgia for a mow strip is 90 mm and the minimum feasible asphalt thickness based on constructability is estimated as 50 mm. Additionally, incorporating the survey results, 25, 50, 90, 125, 175, and 200 mm thick asphalt layers were included in the simulations to show the system response for very thin and very thick mow strips. Similarly, the rear distance values of 0, 150, 300, 600, and 1200 mm were used. Load-displacement curves, ground-level displacement of the post, work done on the system, and the maximum tensile strains in the post flanges were measured.

Development of quantitative assessment criteria

The Roadside Design Guide (AASHTO, 2011), referred to herein as the 'Guide', uses qualitative observations to evaluate the performance of guardrail posts. A guardrail system is considered to exhibit a good performance if a guardrail post is allowed to rotate in the soil, since the post rotation absorbs some of the energy from an impact and reduces the chance of the premature breaking and the plastic hinge formation of the guardrail post. However, the Guide classifies the mow strip as a rigid foundation, which fundamentally precludes assessing the relative impact of mow strip configuration on the behavior of the guardrail system. The experimental and finite element

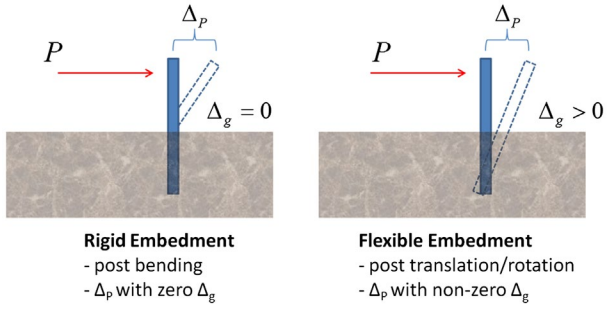

Figure 8. Behavior of guardrail posts in different embedment conditions.

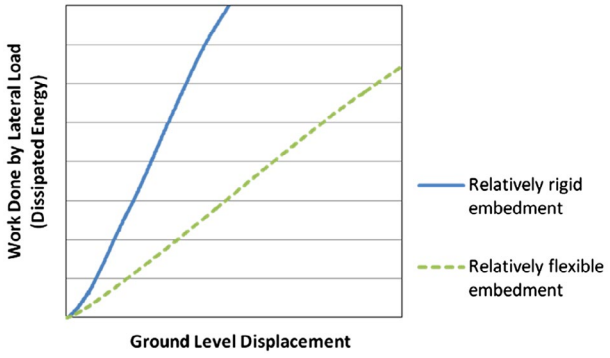

Figure 9. Influence of ground-level displacement on the amount of work done on posts in different embedment conditions.

Table 4. MASH 3-10 crash test condition.

Test condition	Values
Mass of a passenger car (*M*)	1100 kg
Impact velocity (*V*)	27.78 m/s (100 km/h)
Impact angle (θ)	25°
Number of posts[a]	10

[a]Number of posts in minimum length of test section.

analysis results (Figures 6 and 7) indicate that it is more appropriate to consider the asphalt layer as a deformable media, which can result in significant deformation and even failure in the mow strip itself as shown in Figure 7. As such, quantitative assessment criteria should be developed to properly evaluate the relative performance of posts installed with mow strips that have varying geometric or material parameters. The use of quantitative evaluation in lieu of a simple pass/fail criterion also enables a comparison between the structural performance of alternative mow strip configurations and the mow strip incorporating a leave-out recommended in the Guide. These criteria can be used to evaluate the expected relative performance of guardrail posts in mow strips. Thus, post-mow strip combinations which have the best potential to give a satisfactory performance (and those which are more likely not to perform satisfactorily) can be identified using more cost-effective evaluation techniques – such as tests under controlled quasi-static loading.

In this paper, three quantitative assessment criteria have been identified based on the description of desirable post behavior in the Guide: Peak Applied Force, Ground-Level Displacement, and Maximum Post Strain. These criteria are explained by Figure 8, which gives an illustration of the behavior of two laterally loaded posts with significantly different embedment conditions. When a post embedded in a flexible material is subjected to lateral loading, bending of the post is negligible, and the ground-level displacement is proportional to the displacement at the top of the post. On the other hand, when a post is embedded in rigid material such as rock, the post has little ground-level displacement and will exhibit plastic bending as the lateral load exceeds the yield load. The post embedded in a rigid material will therefore carry a higher lateral load and will have a higher longitudinal strain and reduced displacement at the ground level. One simple quantitative indication of relative post performance is to compare these values for different post-mow strip installations.

Peak applied force criterion

The peak force applied to the post is the simplest indicator of potentially excessive restraint of a post-mow strip system. From both the FEA and experimental results, a mow strip setup with thicker and wider rear distance results in a higher peak force. Assuming static equilibrium at the peak load, this creates a higher flexural stress in the post at the ground level. If analysis and test results indicate that an alternative mow strip design gives a similar or lower peak force under static loading than a mow strip design with typical leave-out, the alternative mow strip design may provide a similar level of restraint under dynamic loading.

Ground-level displacement criterion

The ground displacement of the post can also be an indicator of lateral restraint of the system. When two identical posts with varying embedment conditions are subjected to an equal amount of external work in the lateral direction, a post embedded in a relatively rigid material will exhibit less ground-level displacement. Assuming that dissipated energy is equivalent to the amount of work done by the external loading for a closed system, the influence of ground-level displacement of the post on the resulting energy dissipation can be plotted as shown in Figure 9. A smaller slope of the work done vs. ground level displacement, as illustrated by the dashed curve indicates the potential for a relatively desirable performance in the post-mow strip system. A standard dissipated energy level based on the MASH 3-10 crash test condition, as shown

Table 5. FEA and experimental results determined by performance criteria.

Test number	Mow strip thickness (mm)	Mow strip rear distance (mm)	Exp. peak applied force (kN)	FEA peak applied force (kN)	Exp. ground-level displ.[a] (mm)	FEA ground-level displ.[a] (mm)	Exp. max. post strain ratio	FEA max. post strain ratio
B3	0	0	21.1	20.1	211	205	.47	.56
T3	50	600	38.6	37.5	110	117	1.32	1.13
T7	90	600	42.5	41.7	97	90	1.48	1.85
L1–3 (average)	90	600	33.4	–	125	–	.99	–
R1	50	150	28.9	26.3	150	155	.89	.81
R2	50	300	33.1	29.9	129	149	.93	.90
R3	90	300	40.7	34.5	–[b]	146	1.03	1.05

[a]Associated with 7581 J of work done.
[b]Not available due to malfunction of potentiometer during the test.

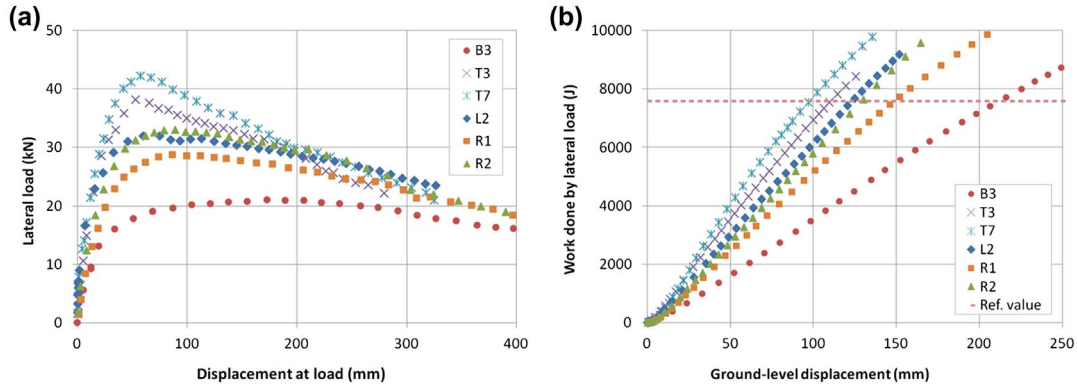

Figure 10. Representative experimental result plots: (a) load vs. displacement, and (b) dissipated energy vs. ground-level displacement.

in Table 4 (AASHTO, 2009), was selected as a reference value to compare computational and experimental results. The lateral kinetic energy (KE) is calculated as follows:

$$KE = \frac{1}{2}MV^2 = \frac{1}{2}(1100\,\text{kg})(27.78\,\text{m/s} \cdot \sin 25°)^2 = 75810\,\text{J} \quad (2)$$

Assuming the lateral kinetic energy is distributed over 10 guardrail posts along the length of the test section, the average dissipated energy (DE_{avg}) on each post can be estimated as 7581 J.

$$DE_{avg} = \frac{KE}{n} = \frac{75810\,\text{J}}{10} = 7581\,\text{J} \quad (3)$$

Maximum strain criterion

The maximum longitudinal strain in the post flanges is a third quantitative indicator of potential excessive restraint of a given post-mow strip system. As seen in Figure 8, a guardrail post embedded in a rigid material undergoes plastic hinging when the load increases beyond the yield load. For simplicity, a normalized maximum strain can be calculated from the maximum strain measured in the post divided by the yield strain. When yielding occurs during the lateral loading test or simulation, the normalized maximum strain exceeds 1.0. If computational analysis and experimental results indicate that an alternative mow strip design results in a similar or lower normalized strain than a mow strip design with a leave-out, the alternative design may provide a similar level of restraint under dynamic loading.

Effect of geometric parameters on the restraint caused by asphalt mow strips

Based on the above rationale, three quantitative criteria can be established to evaluate whether a given post-mow strip configuration, subject to a controlled lateral loading, could potentially provide a similar or lower ground-level restraint compared to a post embedded in a mow strip incorporating a leave-out:

- The post-mow strip system has a similar or higher ground-level displacement at the reference value of external work/dissipated energy compared to a mow strip incorporating a leave-out.
- The post-mow strip system has a similar or lower peak force compared to a mow strip incorporating a leave-out.
- The post-mow strip system has a similar or lower normalized maximum strain compared to a mow strip incorporating a leave-out.

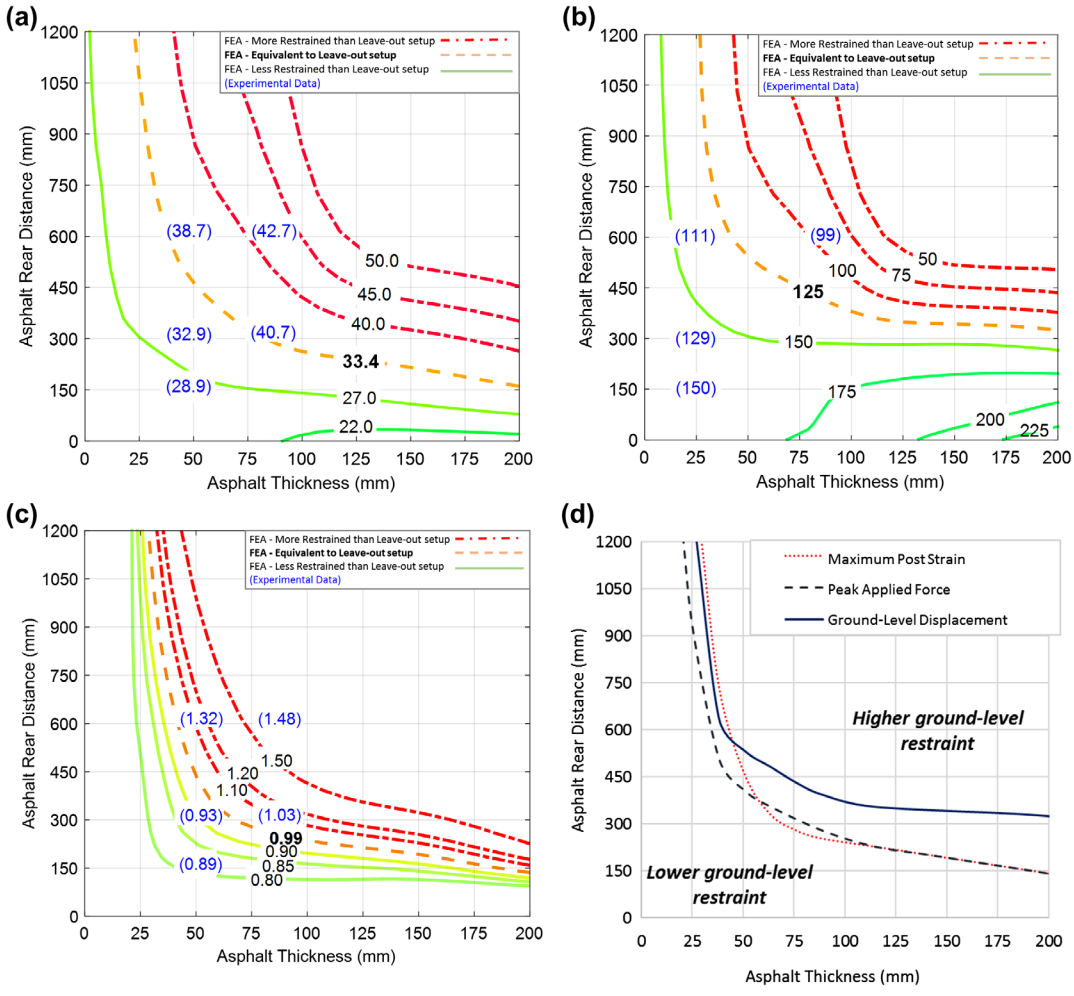

Figure 11. FEA contour plots for combinations of thickness and rear distance: (a) peak applied force (kN), (b) ground-level displacement (mm) associated with 7581 J of work done, (c) normalized maximum post strain, and (d) performance evaluation using all criteria; experimental results given in parentheses.

If a given post-mow strip system does not satisfy any of these criteria, it is reasonable to assume that configuration would result in unacceptable performance not only under quasi-static loading but also under dynamic loading. For a conservative performance assessment, alternative designs were evaluated in service conditions that would be expected to increase the level of restraint on the guardrail post by the mow strip. The lowest ambient temperature recorded during the testing program (10 °C) was selected as the reference temperature for this evaluation. Similarly, the most aged asphalt condition (118 days) experienced in the test program was chosen as the reference age condition of the asphalt.

Table 5 and Figure 10 show the FEA and experimental results related to the three performance criteria. In general, the FEA results show reasonable agreement with the experimental data. From the experiments including the typical leave-out (L1–3), it is apparent that the use of a leave-out reduces the ground-level restraint of guardrail posts compared to the mow strip designs with no leave-out (T7). The average values of leave-out-incorporated design are selected as the target performance values (performance criteria) to assess various mow strip configurations. Obviously, adding any thickness or rear distance of asphalt mow strip increases the restraint compared to the baseline (B3). However, less ground-level restraint can be achieved not only by incorporating a leave-out but also by reducing the thickness (T3), rear distance (R3), or both (R1, R2) of the mow strip.

Using the results of the FEA parametric analyses, contour plots of the three performance assessment criteria were developed to inform whether or not a mow strip design would exhibit less ground-level restraint (preferred alternative designs). Figure 11(a) shows a contour plot of peak force applied to the post, which was created using FEA. Utilizing the FEA model, in conjunction with the experimental program, allows for consideration of a broad range of dimensional (thickness and rear distance)

combinations. The figure demonstrates that a lower peak load can be achieved by reducing asphalt layer thickness, rear distance, or some combination of the two. The 33.4 kN target performance curve of the typical leave-out-applied design is indicated on the contour plot. Values below this reference curve may have satisfactory performance relative to the mow strip configuration incorporating a leave-out. Experimental data from Table 5 and Figure 10(a) are indicated on the plot in parentheses, showing reasonable agreement with the computational results.

Figure 11(b) shows a contour plot of ground-level displacement associated with the reference value of 7581 J work done in the system, which contains a wider range of dimensional combinations than those tested in the experimental program. The 125 mm target performance curve of the typical leave-out-applied designs is indicated on the contour plot. Values below this reference curve may have satisfactory performance relative to the mow strip configuration incorporating a leave-out. Experimental data from Table 5 and Figure 10(b) are indicated in parentheses, showing reasonable agreement with the computational results.

Figure 11(c) shows a contour plot of normalized maximum strain, covering a wider range of thickness-and-rear distance combinations than those tested in the experiment. The .99 target performance curve of the typical leave-out-applied design indicates that any dimensional combination located below this curve may have satisfactory performance relative to the mow strip configuration with typical leave-out. An increase in the thickness or the rear distance induces an additional ground-level restraint as well as higher strains in the post. Experimental data from Table 5 are indicated in parentheses, showing reasonable agreement with the analysis results.

The three contour plots can be combined into one assessment envelope for comparing all three performance assessment criteria. As shown in Figure 11(d), all target performance curves correlate with one another. Since any dimensional combination of asphalt mow strip parameters below these curves is likely to exhibit less ground-level restraint than the reference design, a mow strip configuration which satisfies all three performance criteria can be considered as a potential acceptable alternative to the typical leave-out-applied design. Referring to the mow strip survey result, the following interpretation can be made:

- A mow strip with the nationwide average thickness of 79.5 mm and rear distance of 534 mm is likely to show a higher ground-level restraint than a mow strip incorporating a leave-out.
- A mow strip with the most commonly used thickness of 50 mm and rear distance of 600 mm would show a slightly higher ground-level restraint than a mow strip incorporating a leave-out.

However, an organization can potentially adopt mow strip designs of reduced thickness or rear distance (e.g. R1 configuration with 50 mm thickness and 300 mm rear distance) as an alternative to the mow strip incorporating a leave-out, which would have a satisfactory performance in terms of less ground-level restraint of the post-mow strip system. Mow strip ground-level restrain can also be reduced by applying pre-cuts to the asphalt layer. More details on the use of this method can be found in Lee, Bakhtiary, Stewart, Scott, and White (2016).

Concluding remarks

The ground-level restraint of guardrail posts by various asphalt mow strip designs was investigated using static testing and finite element analysis. Two pertinent geometric parameters of the mow strip – thickness and rear distance – were identified based on a survey of the current practice of mow strip use in the United States. Experimental and FE simulation results were used iteratively: the early phase experiment provided the data for the calibration of FE model, and the FEA simulation was compared to later phase experiments on selected mow strip configurations.

In the experimental program, a static test setup for post-mow strip system was developed to study the behavior of a single post under lateral loading. Multiple mow strip designs were tested under a range of ambient conditions to acknowledge the influence of age and temperature on mow strip restraint. Measured data were utilized for a quantitative assessment of the relative performance of various post-mow strip designs to a common leave-out incorporated design.

In the FEA simulation, the Mohr–Coulomb material models for the soil and the asphalt were calibrated using experimental data. Various modeling attributes, including mesh refinement, nonreflecting boundary condition, hourglass control, contact definition, and element erosion, were scrutinized and implemented to represent the quasi-static load-displacement response of the guardrail post, soil, and asphalt layer system over a large deformation of the post. Parametric studies on targeted geometric parameters were performed and provided the information on expected performance of post-mow strip system.

The FEA and experiment results were integrated under three quantitative performance criteria (Peak Applied Force, Ground-Level Displacement, and Maximum Post Strain) to evaluate the restraint of guardrail posts affected by asphalt mow strips. Decreasing the mow strip thickness and/or rear distance behind the post appears to be an effective way to reduce the restraint imparted by a mow strip on a guardrail system. A range of geometric parameters of desirable performance (less ground-level

restraint) was presented by contour plots that include the target performance curve of the typical leave-out-incorporated design of the AASHTO Roadside Design Guide.

Future work

Future experiments will be performed to evaluate the performance of individual posts installed in a variety of mow strip configurations under dynamic loading using a representative mass and energy programmer. In addition, pertinent properties will also be evaluated via dynamic material testing. The dynamic material test results will be compared to applicable nondestructive assessments of dynamic properties (such as dynamic modulus). These results from the dynamic subcomponent and material tests will be used to refine the finite element models developed for more detailed parametric analysis of the influence of geometric and material properties of the mow strip on the expected performance of the mow strip. The final phase of the research effort will be MASH compliant full-scale crash testing on selected guardrail-mow strip installations to determine whether systems installed without leave-outs can perform satisfactorily.

Disclosure statement

No potential conflict of interest was reported by the authors.

Funding

This research was sponsored by the Georgia Department of Transportation (GDOT) under research project 13-21 'Evaluating the Performance of Guardrail Systems for Installation in Georgia by Driving through Asphalt Layers – Phase I'. Any findings, opinions, recommendations, or conclusions expressed herein are those of the authors and do not necessarily reflect the views of GDOT.

Notes on contributors

David Scott, PhD, is an associate professor in the School of Civil and Environmental Engineering at Georgia Tech. His research interests include the design and evaluation of transportation safety hardware, and the use of novel materials in civil infrastructure.

Lauren K. Stewart, PhD, is an assistant professor in the School of Civil and Environmental Engineering at Georgia Tech. Her research interests include the design and implementation of novel experimental systems for high rate loading environments including blast, shock and impact.

Don White, PhD, is a professor in the School of Civil and Environmental Engineering. His research interests include computational mechanics and applications to the design of civil engineering structures.

Esmaeel Bakhtiary and ***Seo-Hun Lee*** are graduate research assistants and doctoral candidates in the School of Civil and Environmental Engineering at Georgia Tech.

ORCID

Seo-Hun Lee http://orcid.org/0000-0003-1217-705X
Esmaeel Bakhtiary http://orcid.org/0000-0001-8532-5901

References

American Association of State Highway and Transportation Officials. (1993). *Guide for design of pavement structures* (4th ed.). Washington, DC: Author.

American Association of State Highway and Transportation Officials. (2009). *Manual for assessing safety hardware* (1st ed.). Washington, DC: Author.

American Association of State Highway and Transportation Officials. (2011). *Roadside design guide* (4th ed.). Washington, DC: Author.

American Association of State Highway and Transportation Officials. (2012a). *Standard specification for classification of soils and soil-aggregate mixtures for highway construction purposes: AASHTO M 145*. Washington, DC: Author.

American Association of State Highway and Transportation Officials. (2012b). *Standard specification for materials for aggregate and soil-aggregate subbase, base, and surface courses: AASHTO M 147*. Washington, DC: Author.

Arrington, D. R., Bligh, R. P., & Menges, W. L. (2009). *Alternative design of guardrail posts in asphalt or concrete mowing pads* (Report No. 405160-14-1). College Station: Texas Transportation Institute.

Bell, C. A. (1989). *Summary report on aging of asphalt-aggregate systems* (Report No. SR-OSU-A-003A-89-2). Washington, DC: Strategic Highway Research Program (SHRP).

Bligh, R. P., Seckinger, N. R., Abu-Odeh, A., Roschke, P. N., Menges, W. L., & Haug, R. R. (2004). *Dynamic response of guardrail systems encased in pavement mow strips* (Report No. FHWA/TX-04/0-4162-2). College Station: Texas Transportation Institute.

Bowles, J. E. (1996). *Foundation analysis and design* (5th ed.). New York, NY: McGraw-Hill.

Budhu, M. (2010). *Soil mechanics foundations* (3rd ed.). Hoboken, NJ: Wiley.

Christensen, D. W., & Bonaquist, R. F. (2004). *Evaluation of indirect tensile test (IDT) procedures for low-temperature performance of hot mix asphalt: National Cooperative Highway Research Program (NCHRP) report 530*. Washington, DC: Transportation Research Board.

Dewey, J. F., Jeyapalan, J. K., Hirsch, T. J., & Ross, H. E. (1983). *A study of the soil–structure interaction behavior of highway guardrail posts* (Report No. FHWA/TX-83/+343-1). College Station: Texas Transportation Institute.

Eggers, D. W., & Hirsch, T. J. (1986). *The effects of embedment depth, soil properties, and post type on the performance of highway guardrail post* (Report No. FHWA/TX-86/64+405-1). College Station: Texas Transportation Institute.

Farrar, M. J., Turner, T. F., Planche, J.-P., Schabron, J. F., & Harnsberger, P. M. (2013). Evolution of the crossover modulus with oxidative aging. *Transportation Research Record: Journal of the Transportation Research Board, 2370*, 76–83. doi:10.3141/2370-10

Ferdous, M. R., Abu-Odeh, A., Bligh, R. P., Jones, H. L., & Sheikh, N. M. (2011). Performance limit analysis for common roadside and median barriers using LS-DYNA. *International Journal of Crashworthiness, 16*, 691–706. doi: 10.1080/13588265.2011.623023

Fwa, T., Tan, S., & Zhu, L. (2004). Rutting prediction of asphalt pavement layer using C-ϕ model. *Journal of Transportation Engineering, 130*, 675–683. doi:10.1061/(ASCE)0733-947X(2004)130:5(675)

Georgia Department of Transportation. (2015). *GDOT construction standards and details [drawings]*. Retrieved from http://mydocs.dot.ga.gov/info/gdotpubs/ConstructionStandardsAndDetails/Forms/AllItems.aspx

Kulhawy, F. H., O'Rourke, T. D., Stewart, J. P., & Beech, J. F. (1983). *Transmission line structure foundations for uplift-compression loading, load test summaries* (Report No. EL-2870). Palo Alto, CA: Electric Power Research Institute.

Lee, S.-H., Bakhtiary, E., Stewart, L. K., Scott, D. W., & White, D. W. (2016). Effect of pre-cut asphalt fracture planes on highway guardrail performance. *International Journal of Computational Methods and Experimental Measurements, 4*, 353–363. doi:10.2495/CMEM-V4-N3-353-363

Lekarp, F., Richardson, I., & Dawson, A. (1996). Influences on permanent deformation behavior of unbound granular materials. *Transportation Research Record: Journal of the Transportation Research Board, 1547*, 68–75. doi:10.3141/1547-10

Livermore Software Technology Corporation. (2014). *LS-DYNA keyword user's manual: Version 971* (Vols. 1–2). Livermore, CA: Author.

Mak, K. K., Bligh, R. P., & Menges, W. L. (1998). *Testing of state roadside safety systems – Volume XI: Appendix J – Crash testing and evaluation of existing guardrail systems* (Report No. FHWA-RD-98-046). College Station: Texas Transportation Institute.

Pellinen, T. K., Song, J., & Xiao, S. (2004). *Characterization of hot mix asphalt with varying air voids content using triaxial shear strength test*. Paper presented at the 8th Conference on Asphalt Pavements for Southern Africa. Sun City, South Africa.

Plaxico, C. A., Ray, M. H., & Hiranmayee, H. (2000). Impact performance of the G4(1W) and G4(2W) guardrail systems: Comparison under NCHRP Report 350 test 3-11 conditions. *Transportation Research Record: Journal of the Transportation Research Board, 1720*, 7–18. doi:10.3141/1720-02

Ross, H. E., Sicking, D. L., Zimmer, R. A., & Michie, J. D. (1993). *Recommended procedures for the safety performance evaluation of highway features: National Cooperative Highway Research Program (NCHRP) Report 350*. Washington, DC: Transportation Research Board.

Scott, D. W., Lee, S.-H., Bakhtiary, E., Arson, C. F., & White, D. W. (2015). *Static response of steel guardrail posts driven through asphalt vegetation barriers*. Paper presented at Transportation Research Board 94th Annual Meeting. Washington, DC.

Scott, D. W., White, D. W., Stewart, L. K., Bakhtiary, E., & Lee, S.-H. (2015). *Evaluating the performance of guardrail posts installed by driving through asphalt layers* (Report No. 13-21). Atlanta: Georgia Department of Transportation.

Sicking, D. L., Reid, J. D., & Rohde, J. R. (2002). Development of the midwest guardrail system. *Transportation Research Record: Journal of the Transportation Research Board, 1797*, 44–52. doi:10.3141/1797-06

Thom, N. (2013). *Principles of pavement engineering* (2nd ed.). London: ICE Publishing.

United States Army Corps of Engineers (1982). *Bearing capacity of soils: Engineering manual 1110-1-1905*. Washington, DC: Author.

Whitesel, D., Jewell, J., & Meline, R. (2011). *Development of weed control barrier beneath metal beam guardrail* (Report No. FHWA/CA10-0515). Sacramento: California Department of Transportation.

Zhang, Y., Luo, R., & Lytton, R. L. (2013). Characterization of viscoplastic yielding of asphalt concrete. *Construction and Building Materials, 47*, 671–679. doi:10.1016/j.conbuildmat.2013.05.075